Magnetorheology: a review

Juan de Vicente

Departamento de Física Aplicada, Facultad de Ciencias, Universidad de Granada,

18071-Granada, Spain

Correspondence to: Juan de Vicente (E-mail: *jvicente@ugr.es*)

ABSTRACT

Magnetorheology is the branch of Rheology that deals with the deformation and flow behavior of magnetic field-responsive materials. Concretely, magnetorheology studies the rheological consequences of field-induced changes in the mesostructure of colloidal systems. In this contribution we aim to review the fundamental behavior of conventional MR fluids providing a survey on this field.

KEYWORDS

Magnetorheology, magnetic suspension, ferrofluid, magnetorheological fluid, smart material, rheology, colloids

AUTHOR BIOGRAPHIES

Juan de Vicente received Ph.D. degrees in Physics from the University of Granada and the University of Nice-Sophia Antipolis. He has been visitor at the RRC - University of Wisconsin-Madison, Vakgroep Reologie - Universiteit Twente, Unilever Corporate Research and Imperial College London under FPU Predoctoral, and Marie Curie Postdoc, and ERG, Fellowships. He is recipient of the "Young Investigator Award" from the Social Council and the "Physics Research Award" from the Academy of Sciences.

INTRODUCTION

There are some colloidal dispersions that experience dramatic changes in their rheological, magnetic, electrical, thermal acoustic and other mechanical and physical properties when exposed to magnetic fields. For this to occur, at least one phase must be magnetic field-responsive. In most cases, it is the particulate phase that responds to the field (e.g. magnetorheological fluids, ferrofluids) but in other cases it is the carrier fluid that is sensitive to the field (e.g. inverse ferrofluids).

Particles employed in the formulation of magnetorheological (MR) fluids are micron-sized and therefore, they behave as magnetic multidomains. This means that the particles magnetization becomes zero in the absence of magnetic fields. In contrast, superparamagnetic nanosized magnetic particles employed in ferrofluids do remain magnetized even in the absence of magnetic fields. This apparently subtle difference between the particle size in both kinds of field-responsive suspensions determines their macroscopic behavior under fields and eventually the related applications. As a way of example, meanwhile MR fluids may experience a liquid-to-solid transition in the presence of large enough magnetic fields, ferrofluids always remain in the liquid state even in the presence of the field. Figure 1 illustrates the physical mechanism behind the MR effect in *conventional* MR fluids, inverse ferrofluids and magnetic latex suspensions. In this paper we will mostly concentrate on MR fluids where the magnetic phase is the particulate one.

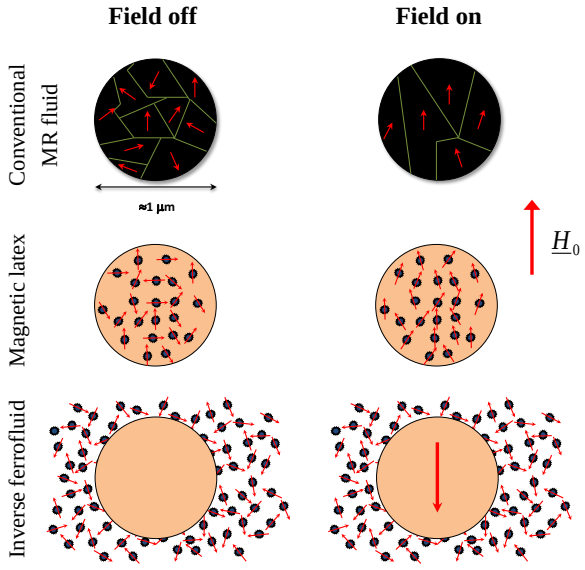

FIGURE 1 - Schematics of the MR effect for the three kinds of MR fluids existing today. Conventional MR fluids are formulated by dispersion of multidomain magnetizable particles in a non-magnetic carrier fluid. Magnetic latexes are dispersions of magnetizable particles, prepared by embedding superparamagnetic particles in a non magnetic colloidal matrix, in a non-magnetic carrier. Inverse ferrofluids consist of dispersions of non-magnetic particles in a ferrofluid. Left: in the absence of magnetic fields. Right: in the presence of magnetic fields.

MR fluids were discovered in 1948 by Jacob Rabinov[1], inspired by a seminar at the US National Bureau of Standards on Electrorheological (ER) fluids by Willis M. Winslow[2]. Serious difficulties in stabilizing MR fluids impeded a rapid commercial success in the years following the development and most of the research continued focused on ER fluids. However, a revival of interest in magnetorheology was experienced in 1990's, and MR fluids are nowadays clearly preferred over ER fluids, because the former possess much stronger field-induced interparticle forces. Actually, the strength (i.e. *yield stress*) is around one order of magnitude larger in the case of MR fluids (for typical magnetic field strengths of approx. 1 kOe) than ER fluids (for typical electric field values of approx. 1 kV/mm). Complete reviews of MR fluids can be found in refs[3-9].

The ability to control the rheological properties of MR fluids has found numerous applications that can be safely classified in three groups: torque-transfer applications, damping applications and process applications. Currently, MR technology is applied in shock absorbers, engine mounts, clutches, brakes, control valves, actuators and artificial joints among others[7,10].

In spite of the large progress in this field, MR fluids do not still satisfy the diverse and stringent requirements demanded in commercial applications. For instance, the maximum MR effect is limited (by the saturation magnetization of the magnetic phase). Also the response, although quick, is restricted by the ratio between the inductance of the coils and their resistance. The magnetic phase frequently exhibits remanence. This means that the phase remains slightly magnetized even when the magnetic field is removed. As a consequence, the relaxation is typically smaller and also redispersibility issues arise. Finally, the density of the magnetic phase is significantly different from the non-magnetic phase resulting in the long-term sedimentation of the colloid.

The paper is organized as follows. In the next section we briefly recall some definitions and laws of magnetism that are relevant in magnetorheology. Next, the MR effect is explained in terms of the Particle Magnetization Model. Dimensionless numbers are introduced in the following section. The basics on the formulation of MR fluids is summarized next. Subsequently, the main rheological properties and their dependence with particle concentration and field strength are discussed under the frame of analytical theories and particle level simulations. The paper ends with some applications.

REVIEW ON MAGNETISM

The magnetic properties of matter have their origin in the electric charges moving inside atoms and molecules: by the orbiting of electrons around the nuclei and by the electrons spinning on their axes. The movement of these charges creates current loops that can be considered as magnetic dipoles with a magnetic moment associated $\underline{m}$. In general these moments cancel each other. However, in the presence of a magnetic field the matter becomes magnetized[11].

The magnetization (per unit volume) of matter $\underline{M}$ is proportional to the number of magnetic moments per unit volume and the dipole magnetic moment $\underline{m}$. The magnetization depends on the magnetic properties of the material and the internal magnetic field $\underline{H}$ through the following equation

$$\underline{M} = \chi \underline{H} \tag{1}$$

where χ is the magnetic susceptibility.

The magnetic induction of matter is expressed by:

$$\underline{B} = \mu_0 \left(\underline{H} + \underline{M} \right) = \mu_0 \mu_r \underline{H} \tag{2}$$

where $\mu_r = 1 + \chi$ in the relative magnetic permeability of the material and μ_0 is the permeability of free space ($\mu_0 = 4\pi \times 10^{-7} N / A^2$).

The field inside matter $\underline{H}$ is different from the external magnetic field $\underline{H}_0$. This is so because the external magnetic field induces a magnetization of matter that eventually acts as a source of another field $\underline{H}_D$ that opposes to the external field. This field is the so-called demagnetizing field and depends on the permeability of the material and also on its shape. With this, the internal magnetic field is written as:

$$\underline{H} = \underline{H}_0 + \underline{H}_D = \underline{H}_0 - N_D \underline{M} \tag{3}$$

where N_D is the demagnetizing factor and depends on the material shape only. For the particular case of a sphere, $N_D = 1/3$.

For a sphere with relative magnetic permeability μ_{pr}, dispersed in a continuum medium of relative permeability μ_{cr}, the internal magnetic field in the particle reads $H = \dfrac{3\mu_{cr} H_0}{\mu_{pr} + 2\mu_{cr}}$ and therefore the magnetization of the sphere becomes $M = 3\beta H_0$. Here, $\beta \equiv \dfrac{\mu_{pr} - \mu_{cr}}{\mu_{pr} + 2\mu_{cr}} = \dfrac{\alpha - 1}{\alpha + 2}$ essentially defines the ratio between the magnetic permeability of the particles and that of the continuous phase.

In the formulation of conventional MR fluids, dispersed particles are constituted by strongly ferromagnetic materials because they have a very large (in magnitude) magnetization, so the magnetic flux density through them is a great deal larger than that of free space. In particular, the preferred choice is carbonyl iron. The magnetic properties of carbonyl iron particles are well described by the Frohlich-Kennely equation:

$$M = \frac{\mu_i H}{1 + \frac{\mu_i}{M_s} H} \tag{4}$$

Typical values for the relative initial permeability and saturation magnetization are $\mu_i = 100$ and $M_s = 1400\,\mathrm{kA/m}$, respectively. At low fields, M is proportional to H. With increasing the magnetic field strength the magnetization begins to saturate eventually reaching the saturation magnetization M_s.

PHYSICAL MECHANISM

There is only one widely accepted mechanism proposed to account for the MR effect. This is the so-called Particle Magnetization Model[9]. When a conventional MR fluid is subjected to the presence of a magnetic field, particles become magnetized. At low fields and under the assumption that the particles are spherical in shape and monodisperse in size with diameter a, the field-induced magnetic moment, m, becomes:

$$m = 4\pi\mu_0\mu_{cr}\beta a^3 H_0 \tag{5}$$

Eq. (5) is only valid at low fields, well in the linear regime. On the other extreme, at very large fields, in the saturation regime, the magnetic moment of the particles is constant and can be written as follows:

$$m = \frac{4}{3}\pi\mu_0\mu_{cr} a^3 M_s \tag{6}$$

Once the particles become magnetized under the field, they interact through magnetostatic forces that are given by the following expression:

$$\underline{F}_{ij}^{mag} = (\underline{m}\cdot\nabla)\underline{B} \tag{7}$$

Neglecting local field corrections, the magnetic interaction force in dipolar approximation reads:

$$\underline{F}_{ij}^{mag} = -\frac{3m^2}{4\pi\mu_0\mu_{cr} r_{ij}^4}\left[\left(3\cos^2\theta_{ij} - 1\right)\hat{r} + \sin\left(2\theta_{ij}\right)\hat{\theta}\right] \tag{8}$$

where, r_{ij} is the center-to-center distance between the particles and θ_{ij} the angle between the center-to-center vector and the magnetic field vector (see Figure 2).

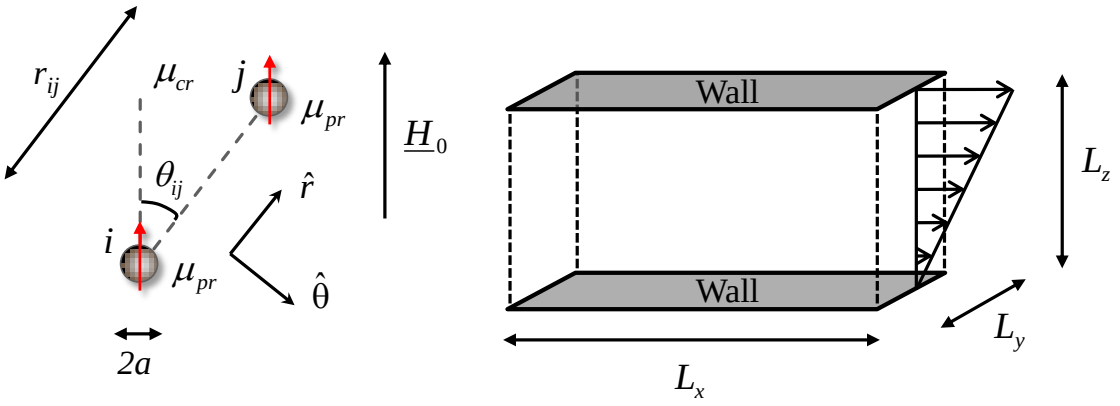

FIGURE 2 - Coordinate system for a pair of particles in the presence of a magnetic field undergoing a shearing deformation.

Substituting Eq. (5) in Eq. (8) we get the expression for the bare point dipole force (and interaction energy) for two isolated spheres having the same strength m:

$$\underline{F}_{ij}^{mag} = -12\pi\mu_0\mu_{cr}\beta^2 a^2 H_0^2\,\underline{f}; \quad \underline{f} = \left(\frac{a}{r_{ij}}\right)^4\left[\left(3\cos^2\theta_{ij}-1\right)\hat{r}+\sin\left(2\theta_{ij}\right)\hat{\theta}\right] \tag{9a}$$

$$V_{ij}^{mag} = \frac{m^2}{4\pi\mu_0\mu_{cr}r_{ij}^3}\left(1-3\cos^2\theta_{ij}\right) \tag{9b}$$

Eqs. (9) clearly reveal that the magnetostatic interaction force is long-ranged in marked contrast to other colloidal forces. Furthermore it is strongly anisotropic (see Figure 3). For $\theta_{ij} < 55^o$ the radial component of the magnetic interaction force will be attractive. In contrast, for $\theta_{ij} > 55^o$ particles will repel each other. Finally, it is worth to remark that the magnetic interaction force at low field is essentially proportional to the magnetic field strength squared.

Eq. (9) also gives a qualitative explanation of many of the rheological observations in magnetorheology, especially at low particle concentrations. However, when attempting to obtain quantitative agreement, this point-dipole approximation fails because of the presence of multibody and multipolar interactions that are not considered in this approximation[12,13]. Understanding the behavior of concentrated suspensions constitutes a formidable challenge and requires further investigations. It is expected that in highly concentrated MR fluids, colloidal (short-range) forces come into play.

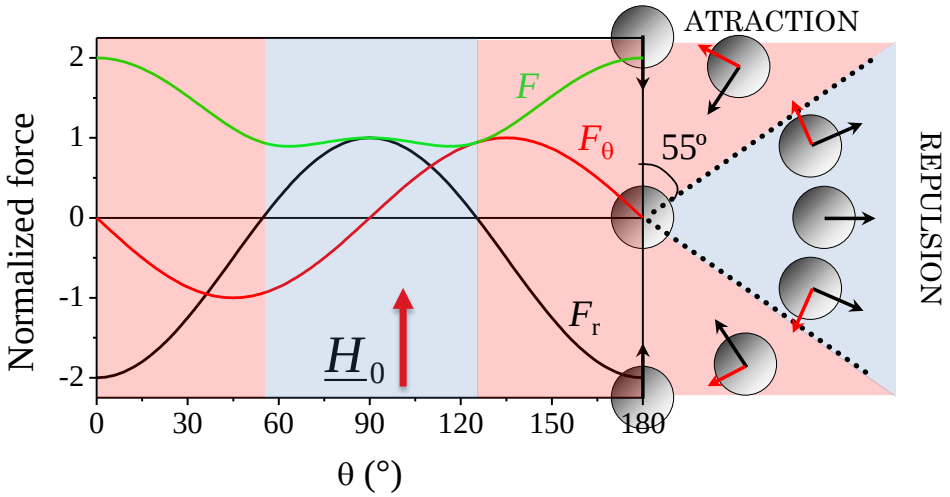

FIGURE 3 - Dipolar interaction force between two isolated magnetizable spherical particles. Particles whose separation is perpendicular to the field repel each other, while those whose separation is parallel to the field attract.

DIMENSIONLESS NUMBERS IN MAGNETORHEOLOGY

Apart from other dimensionless numbers used in conventional colloidal dispersions, such as the particle volume fraction, Reynolds and Peclet number, in magnetorheology we need two more: the dipolar coupling parameter and the Mason number.

The dipolar coupling parameter (or magnetic Peclet Number), λ, gives a relation between the magnetic and thermal energies acting on a MR fluid. It is frequently defined as the ratio between the magnetic dipolar energy of two parallel dipoles separated a distance $2a$ and the thermal energy:

$$\lambda = \frac{\pi \mu_0 \mu_{cr} \beta^2 a^3 H_0^2}{2 \kappa_B T} \tag{10}$$

Here κ_B is the Boltzmann constant and T is the absolute temperature. For micronsized particles at room temperature under typical magnetic fields (> 1 Oe), the magnetic forces dominate the Brownian force and therefore $\lambda >> 1$.

Other dimensionless number that applies under flow conditions is the so-called Mason number. For steady simple shear, it is defined as the ratio between stokesian hydrodynamic force acting on a particle due to the shear and the magnetostatic interaction force between two parallel dipoles in close contact:

$$Mn = \frac{8 \eta \dot{\gamma}}{\mu_0 \mu_{cr} \beta^2 H_0^2} \tag{11}$$

Here η is the steady shear viscosity, and $\dot{\gamma}$ is the magnitude of the shear rate tensor.

Importantly, for MR fluids where inertia and Brownian motion can be safely neglected, rheological material functions under flow (e.g. shear viscosity) are demonstrated to solely depend on the particle volume fraction ϕ, the dipolar coupling parameter λ and the Mason number Mn[3].

PREPARATION OF MR FLUIDS

The composition of a typical MR fluid can be broken into three parts: magnetic particles, a carrier fluid and additives[14-16]. Although model MR fluids generally comprise only the particles and a liquid, a good performance under application definitely requires an assortment of additives. Magnetic particles constitute a total of 20-40 % by volume of the total fluid. They are typically carbonyl iron because of its high saturation magnetization (2.1 T) and high purity (> 99.5 %). It has been reported that more than 90 % of the raw material cost comes from the carbonyl iron powder used in the formulation of commercial MR fluids. Common carrier fluids include silicone oils, water, petroleum based oils, mineral oils and synthetic hydrocarbon oils such as poly(alpha-olefins). By far, the most common dispersing liquid are hydrocarbon oils. They must be stable over the range of operating pressures and temperatures in the intended application. Finally, additive agents are also included in the formulation to improve the redispersibility, kinetic stability against aggregation and sedimentation, and to lubricate the particles. Suspension agents include organoclays, carboxylated soaps, fumed silicas and surfactants among others. All in all, the composition details of a MR fluid strongly depends on its particular application.

RHEOLOGICAL BEHAVIOR

The performance of a MR fluid is typically judged by the magnitude of its field-induced yield stress as it measures the strength of the material. In conjunction with a large yield stress under the field, it is equally important to maintain a low off-state viscosity. This is typically expressed as the turn-up ratio or relative MR effect that is defined as the ratio between the viscosity increment under field and the viscosity value in the absence of the field[7].

The yield stress is an engineering reality that can be defined as the minimum stress value to the onset of flow. However, there is currently a hot debate on whether a true yield stress exists or not using fundamental principles[17-19]. The reason for this stems from the fact that measurements are necessarily done over finite periods of time and therefore, resulting data depend on the scale of time explored. This means that the same MR fluid can be considered a yield stress material when measured at short time scales but in contrast it could behave as a liquid when measuring over longer times (Figure 4). It is well known today that this time-dependency is closely associated to the thixotropic behavior of the material[20].

Even though, there is currently a great interest in the understanding of the flow behavior of MR fluids under non-shearing more complex elongational flows, the steady shear flow behavior is the one that has received larger attention in the past probably due to the fact that it is easier to superimpose well-controlled magnetic fields to it. Actually, the shear flow behavior of MR fluids is generally well described by the Bingham constitutive equation that reads as follow[21]:

$$\tau = \tau_0 + \eta_p \dot{\gamma} \tag{12}$$

where τ_0 is the (magnetic field-dependent) yield stress and η_p represents the (field-independent) plastic viscosity.

In dimensionless form, the Bingham equation can be written using the Mason number as follows:

$$\eta/\eta_\infty = 1 + \left(Mn/Mn^*\right)^{-1} \tag{13}$$

Here, Mn^* is the critical Mason number that determines the transition from magnetization to hydrodynamic control of the suspension structure.

Primitive models in magnetorheology assume a cubic network of infinite single-width chains of particles, arranged in a line with respect to the field direction, that deform affinely with the flow field. These models predict a Bingham plastic behavior with a yield strain around ~10 % (cf. Eqs. 12 & 13)[21-25]. However, a careful look to the low shear regime reveals that experimental data do better fit the Casson plastic model instead of the Bingham model[17,26,27]. The reason for this comes from the coupling between the hydrodynamic and magnetostatic stresses that eventually result in a smoother transition from a solid to liquid state under increasing stresses. Also important is to note that for "weak" MR fluids (i.e. inverse ferrofluids) a low shear viscosity plateau has been reported in the literature that is in clear disagreement with a plastic model (either Bingham or Casson)[28]. Experiments reveal that weak MR fluids do behave as high viscosity liquids at low shear instead of pure elastic solids as predicted by the Bingham model (see Figure 4). Recently, a structural viscosity model has been proposed that explains these two deviations from the Bingham model predictions[17]. Furthermore, this structural model has been also extended to explain time dependence of MR fluids under an aging-rejuvenation framework[20].

The structural viscosity model predicts a shear viscosity that scales with Mason number as follows[17]:

$$\frac{\eta}{\eta_\infty} = \left[\frac{1 + \left(Mn/Mn^*\right)^{1/2}}{\left(\eta_\infty/\eta_0\right)^{1/2} + \left(Mn/Mn^*\right)^{1/2}}\right]^2 \tag{14}$$

where η_0 (η_∞) is the low (high) shear viscosity. This model explains well the behavior of inverse ferrofluids[17].

When interparticle magnetic interactions are very strong, as is the case of conventional MR fluids, the low shear viscosity plateau value (if exists) is exceedingly large and actually it is hardly observed within the experimental time scales typically explored. As a consequence, an apparent yield stress and a plastic-like behavior come up. Such a plastic constitutive equation can be derived by expanding Eq. (14) for $\eta_0 >> \eta_\infty$. With this, we get the Casson plastic equation:

$$\eta/\eta_\infty = 1 + \left(Mn/Mn^*\right)^{-1} + 2\left(Mn/Mn^*\right)^{-1/2} \tag{15}$$

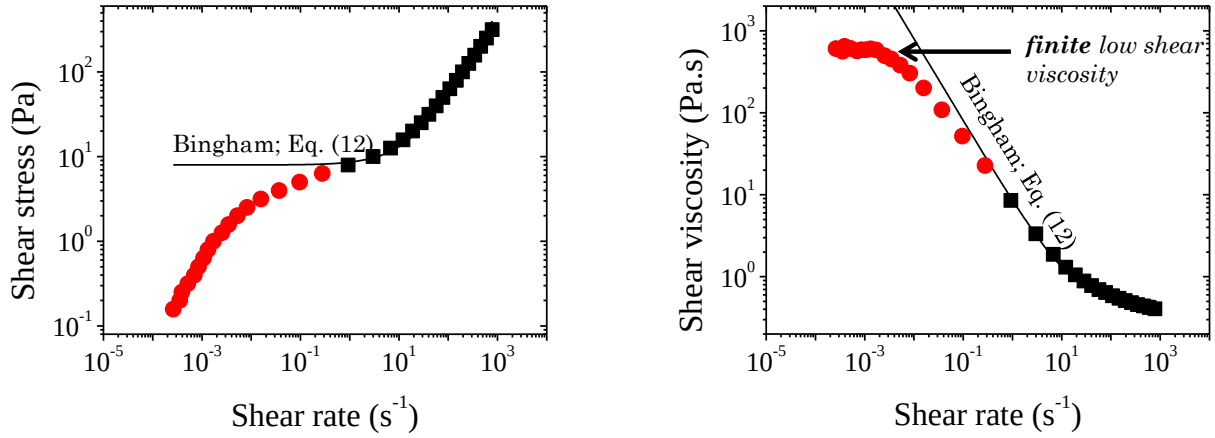

FIGURE 4 - Typical steady shear flow experiment for MR fluids. Left: rheogram, Right: viscosity curve. Black squares are measured at short time scales. Red circles are typically obtained for long acquisition times in the case of inverse ferrofluids. Experimental data correspond to a 25 vol% silica-based inverse ferrofluid in the presence of a external magnetic field of 265 kA/m.

The Casson plastic equation (Eq. 15) is capable to explain the more gradual transition from the yield to the Newtonian region for conventional MR fluids both in the liquid region and in the solid region for concentrations up to 50 vol%. As a way of example, in Figure 5 we compare the predictions of the Casson model with results obtained in highly concentrated MR fluids.

Generally speaking, the yield stress can be increased by either increasing the particle concentration or increasing the external magnetic field strength. At low particle contents, the yield stress is proportional to the concentration as expected from micromechanical models based on single-width particle chains. However, upon further increasing the concentration a faster than linear increase is observed. Here, colloidal gel approaches are claimed to provide a quantitative explanation [see ref [18] and references therein].

The effect of magnetic field strength on the yield stress of conventional MR fluids is well documented in the literature[29]. At low fields, $\beta \approx 1$, and the yield stress increases quadratically with the field strength as expected from the Particle Magnetization Model $\tau_0 \approx \phi\mu_0 H_0^2$. When the field strength increases,

the field dependence diminishes as a result of the saturation of the magnetization within the particles. At this stage $\tau_0 \approx \phi\mu_0 M_s^{1/2} H_0^{3/2}$. Finally, for very large fields, particles fully saturate and therefore, the yield stress reaches a maximum value $\tau_0 \approx \phi\mu_0 M_s^2$.

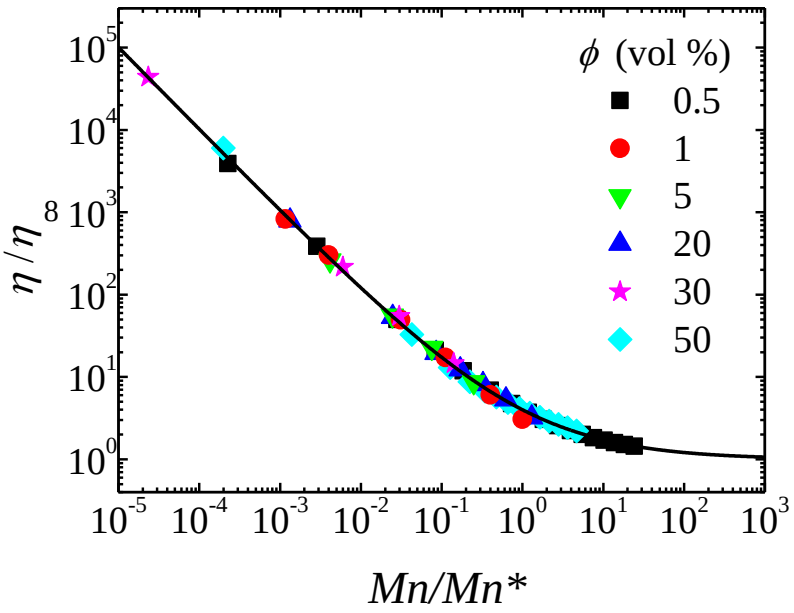

FIGURE 5 - Dimensionless viscosity as a function of the reduced Mason number for a conventional MR fluid prepared by dispersion of micronsized carbonyl iron microparticles (from BASF SE, Germany) in 20 mPa.s silicone oils at different concentrations. The field strength is 88 kA/m. The solid line represents the Casson model prediction (Eq. (15)).

In the last few decades, the number of unsteady shear flow investigations has significantly increased. With the advent of extremely sensitive rheometers, the (very-narrow) linear viscoelastic behavior of MR fluids (below 0.01-0.1 %) has become accessible using small amplitude oscillatory shear[30,31]. Special emphasis has been paid to the understanding of the field dependence of the storage modulus G' in the "solid-like" regime. Under magnetic fields, the storage modulus is reported to increase quadratically with the magnetic field strength $G' \approx \phi\mu_0 H_0^2$. For intermediate fields, particles begin to saturate and therefore a subquadratic dependence is found $G' \approx \phi\mu_0 M_s H_0$. At exceedingly large fields, particles fully saturate and the storage modulus becomes independent of the magnetic field strength $G' \approx \phi\mu_0 M_s^2$.

The unsteady shear flow behavior of MR fluids is better investigated using creep-recovery experiments[20]. These experiments reveal that MR fluids only behave in the linear viscoelastic regime when subjected to

extremely low stress levels. Rheomicroscopy investigations demonstrate that gap-spanning structures stretch still connecting the plates under shear at these stress values. When the stress is ceased, the deformation is fully recovered. When further increasing the stress level, a plastic contribution to the resulting strain appears that is associated to the appearance of non-gapspanning structures and to irreversible microstructural rearrangements. When the stress value approaches the yield stress, a fully plastic fluid behavior is exhibited and the sample does not recover at all when the stress is removed. For very large stresses, the MR fluid flows with a very low viscosity level. Typical creep-recovery experiments for conventional MR fluids at different stress levels are included in Figure 6. The low stress behavior has been reported to be very similar to the one of highly thixotropic clay suspensions. In contrast, the high shear stress regime looks more alike to non-thixotropic microgel suspensions.

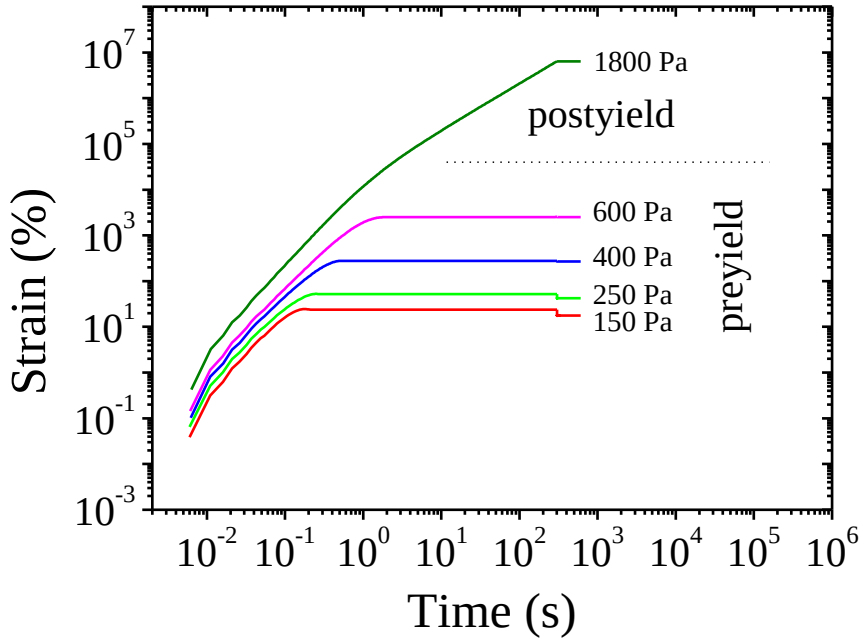

FIGURE 6 - Time dependence of the shear strain achieved during a step stress (creep) and recovery experiment at a 5 vol% carbonyl iron MR fluid for several stresses as indicated in the figure. The magnetic field strength is 173 kA/m.

Current applications typically subject the MR fluids to very demanding conditions where driving surfaces are very close to each other and therefore, deformation rates are exceedingly large. Depending on the particular application, the corresponding shear rates can be as large as 10^4 s^{-1} (as found in the MotionMaster damper[32]) or even higher, as is the case of the MR-based suspension for the Army's HMMWV Hummer[33]. As a result, conventional rheological techniques do not provide useful information to understand the behavior of these fluids under these extreme flow conditions, and a tribological approach is needed[34].

PARTICLE LEVEL SIMULATIONS IN MAGNETORHEOLOGY

Non-Brownian dynamic simulations are useful tools for the investigation of the rheological properties of MR fluids. Since an external force is applied to the system, this becomes non-equilibrium in nature[12,35-39]. MR fluids are typically modelled as a collection of N non-Brownian, buoyant, equal sized spheres (radius a) with relative magnetic permeability μ_{pr} confined between two parallel walls. The continuous phase is a Newtonian fluid of viscosity η_c and relative magnetic permeability μ_{cr}. An external magnetic field (parallel to the vertical *z*-axis) is applied to promote the structuration. Periodic conditions are assumed in *x*- and *y*- directions. The configuration of the system and the coordinate description is shown in Figure 2.

The trajectories of the particles are typically determined solving Langevin motion equation under the assumption that Brownian forces are negligible. For any particle *i* in the system it may be written as:

$$m_p \frac{d^2 \underline{r}_i}{dt^2} = \sum \underline{F}_i, \qquad i = 1,2,...,N \tag{16}$$

where m_p is the mass of the particle, $\underline{r}_i$ is the position vector of the *i*th particle, $\underline{F}_i$ is any force exerting on the particle, and *N* is the total number of particles. It is important to note here that in order to solve this equation, all forces on *i* must be considered.

To describe the long range magnetostatic interaction between micron-sized spheres it is frequently employed the so-called bare point-dipole model (Eq. 9a). Accordingly, particles are magnetized in the presence of a magnetic field due to the mismatch in the permeability between the particles and the dispersing medium. Assuming pairwise additivity, the magnetic force on particle *i*, $\underline{F}_i^{mag}$, may be written as:

$$\underline{F}_i^{mag} = \sum_{j \neq i,\, j=1}^{N} \underline{F}_{ij}^{mag} = \sum_{j \neq i,\, j=1}^{N} F_0 \left(\frac{2a}{r_{ij}} \right)^4 \left[\left(3\cos^2 \theta_{ij} - 1 \right) \hat{r} + \left(\sin 2\theta_{ij} \right) \hat{\theta} \right] \tag{17}$$

where $F_0 = \frac{3}{4} \pi \mu_0 \mu_{cr} \beta^2 a^2 H_0^2$ is the force normalizing factor.

Short-range repulsive forces are typically used to mimic the sphere-wall interactions and to prevent particles from overlapping. A frequent choice is a quasi-hard sphere repulsion modeled as an exponential decay:

$$\underline{F}_i^{rep} = \sum_{j \neq i,\, j=1}^{N} -F_0 \exp\left[-100 \left(\frac{r_{ij}}{2a} - 1 \right) \right] \hat{r} \tag{18}$$

Many-body effects are generally discarded to reduce computational complexity when simulating hydrodynamic forces acting on the particles. The drag force acting on an isolated particle due to laminar viscous fluid flow is given by Stokes formula:

$$\underline{F}_i^{hydr} = -3\pi\eta_c d\left[\frac{d\underline{r}_i}{dt} - \underline{v}_i\right] \tag{19}$$

where $\underline{v}_i$ stands for the ambient fluid velocity at the particle center.

Computer simulations are performed using reduced units. The parameter values used in the simulations are generally:

$$F_0\,; \qquad l_0 = 2a\,; \quad t_0 = \frac{12\pi\eta_c a^2}{F_0} \tag{20}$$

Hence, using reduced units and neglecting inertia, the equation of motion (Eq. 16) can thus be written in dimensionless form as follows:

$$\frac{d\underline{r}_i^*}{dt^*} = \underline{F}_i^{mag*} + \underline{F}_i^{rep*} + \underline{v}_i^* \tag{21}$$

Numerical integration of Eq. 21 provides the positions of the particles and therefore, the stress tensor components can be evaluated. In particular, the instantaneous magnetostatic contribution to the shear stress, τ_{mag}^*, can be calculated as the sum of restoring forces against the imposed shear flow according to the Kirkwood formula:

$$\tau_{mag}^* = -\frac{1}{L_x^* L_y^* L_z^*}\sum_{i=1}^{N} z_i^* F_{ix}^* \tag{22}$$

where F_{ix}^* is total dimensionless magnetostatic plus short-range repulsive force acting on sphere *i* in the *x*-th direction and $L_x^* L_y^* L_z^*$ is the volume of the system.

Similarly, the viscous contribution to the stress is typically given by:

$$\tau_{vis}^* = \frac{1}{3\pi}\left(1+\frac{5}{3}\phi\right)\dot{\gamma}^* \tag{23}$$

As a consequence, as a first approximation, the total stress, τ^*, can be written as:

$$\tau^* = \tau_{mag}^* + \tau_{vis}^* \tag{24}$$

Recalling Eq. 12, the yield stress τ_0 is controlled by the first term in Eq. 24, while the plastic viscosity η_p is controlled by the second term in Eq. 24. The simplified description assumed above is only really valid in the case where the permeability ratio α is small and for widely separated particles where point-dipole and stokes'-drag equations hold. In practice, particle concentrations are particularly high and therefore, the analysis becomes significantly complex. Many-body, polidispersity, and transient responses have also been simulated in the literature[12,13,40-42]. In these analyses, the mutual polarization of the particles is considered self-consistently, and is found to increase with the enhancement of the particle concentration and the permeability ratio between the solvent and the particles. Even if multipoles are taken into account, the scaling of the force with the field strength and particle size are still given by the dipole results.

Traditionally, components of the stress tensor other than the shear stress have excited little interest. However, with the introduction of new rheometers that are capable to measure the normal forces under shear, the number of papers covering this important aspect has increased. MR fluids tend to exhibit a quadratic dependence of the static (no-shear) normal force with the magnetic field strength. For stresses slightly larger than the yield stress, the normal force typically decreases[43-46].

APPLICATIONS

Probably, the most popular application of MR fluids concerns its use in semi-active dampers for the automotive industry[7,47,48]. The benefit of using MR fluids instead of conventional oils stems from their large dynamic forces combined with very rapid mechanical responses. Furthermore, MR dampers do not require mechanical valves to restrict flow contrary to hydraulic dampers. A schematic representation of a MR damper is shown in Figure 7. The automotive suspension system, MagneRide, first incorporated MR technology in the Cadillac Seville STS as early as 2002. An improved version of that vehicle primary suspension system is currently used as a standard suspension or an option in many models for Cadillac, Buick, Chevrolet, Holden Special Vehicles, Ferrari and Audi.

MR fluids are also used in rotary brakes to be used in exercise equipment, pneumatic actuators and steer-by-wire systems. Vehicle secondary suspensions do also benefit from MR devices. An example is the Rheonetic RD-1005-3 MR damper manufactured by Lord Corporation. MR dampers are also used in civil engineering applications, for seimic protection and cable stayed bridges, and biomedical applications (e.g. prosthetic leg developed by Biedermann Motech GmbH). Also relevant is the use of MR fluids in the polishing of optical lenses (QED technologies) and impact or shock loading applications (e.g. active recoil of large caliber gun systems and bullet-proof vests).

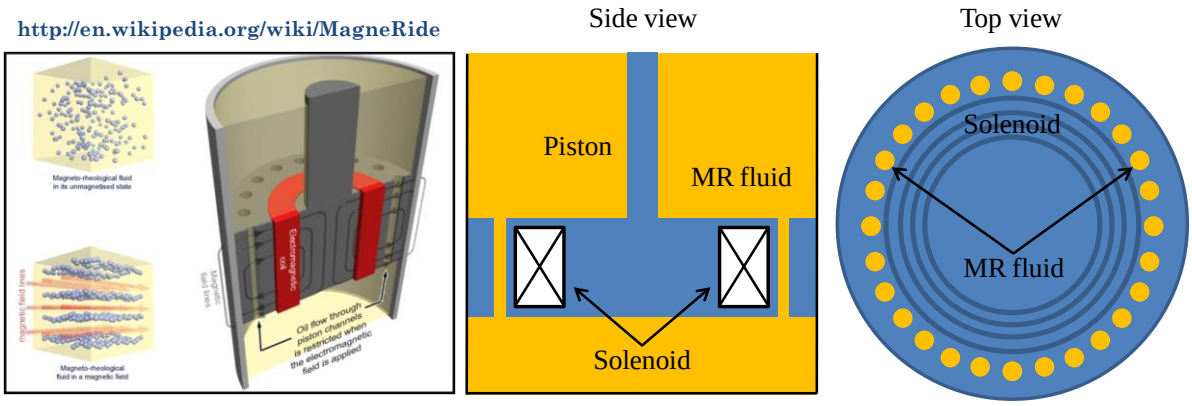

FIGURE 7 - Functional principle of the MagneRide MR damper.

Generally speaking MR fluid applications typically involve one of three different modes or combinations of them: valve mode, shear mode and squeeze mode. In valve mode the fluid is confined by stationary surfaces and made to flow under a pressure gradient. In the shear mode, the fluid flows between two flat surfaces sliding relative to each other. Finally, in the squeeze flow mode the fluid is either compressed or stretched between two surfaces. Shear mode appears in MR brakes and clutches, while MR dampers subject the fluids to both valve and shear deformations. Small amplitude vibration mitigation involves squeeze flow deformations. Most of the scientific literature on MR fluids concentrate on shearing flows. However, there is currently a large interest in a better understanding of the behavior of MR fluids under valve and squeeze flow modes[49-55].

CONCLUSIONS

MR fluids are examples of smart materials that are interesting both from a fundamental and practical approach. On the one hand, they can serve as model colloidal materials for fundamental studies regarding gelation and aggregation processes as the interparticle interaction can be externally controlled. In fact, they are probably the colloidal materials exhibiting the largest possible interparticle interactions. On the other hand, their field-dependent yield stress and the fast response time has made MR fluids an attractive technology for many commercial applications. Research efforts in the past have focused on providing a better understanding of the steady shear flow properties and specially the non-linear yielding behavior. The Particle Magnetization Model explains well the behavior of particularly dilute suspensions where analytical approaches and particle-level simulations (neglecting inertia and Brownian motion) apply.

ACKNOWLEDGEMENTS

This work was supported by MICINN MAT 2010-15101 project (Spain), by the European Regional Development Fund (ERDF) and by Junta de Andalucía P10-RNM-6630 and P11-FQM-7074 projects (Spain).

REFERENCES AND NOTES

1. Rabinow, J., *AIEE Trans*,**1948**,*67*,1308.
2. Winslow, W.M., J. Applied Physics,**1949**,*20*,1137-1140.
3. Gast, A. P.; Zukoski, C. F., *Adv. Colloid Interface Sci.*,**1989**,*30*,153.
4. Ginder, J. M. *MRS Bulletin*,**1998**,*23*,26.
5. See, H. *Applied Rheology*,**2001**,*11*,70.
6. Bossis, G.; Volkova, O.; Lacis, S.; Meunier, A. in Ferrofluids: Magnetically Controllable Fluids and Their Applications, Lecture Notes in Physics Vol. 594, edited by S. Odenbach, Springer-Verlag, Berlin, **2002**, 202–230.
7. Goncalves, F. D.; Koo, J. -H.; Ahmadian, M., *The Shock and Vibration Digest*,**2006**,*38*,203-219.
8. Park, B. J.; Fang, F. F.; Choi, H., J. *Soft Matter,***2010**,*6*,5246-5253.
9. de Vicente, J.; Klingenberg, D. J.; Hidalgo-Álvarez, R., *Soft Matter*,**2011**,*7*,3701-3710.
10. Klingenberg, D. J., *AIChE Journal*,**2001**,*47*,246-249.
11. Bozorth, R. M., Ferromagnetism; R. M. Bozorth, Ed.; van Nostrand: Toronto, Canada, **1951**.
12. Klingenberg, D. J.; van Swol, F.; Zukoski, C. F., *J. Chem. Phys.,***1991**,*94*,6170.
13. Bonnecaze, R. T.; Brady, J. F., *J. Chem. Phys.,***1992**,*96*,2183.
14. Foister, R. T.; Iyengar, V. R.; Yurgelevic, S. M., US Patent 6,687,058.
15. Phule, P. P., *MRS Bulletin*,**1998**,*23*,23-25.
16. Bombard, A. J. F., Antunes, L. S.; Gouvêa, D., *J. Phys. Conf. Series,***2009,***149*,012038.
17. Berli, C. L. A.; de Vicente, J., *Appl. Phys. Lett.*,**2012**,*101*,021903.
18. Segovia-Gutiérrez, J. P.; Berli, C. L. A.; de Vicente, J., *J. Rheol.*,**2012**,*56(6)*,1429-1448.
19. Rodríguez-López, J.; Elvira, L.; Montero de Espinosa Freijo, F.; Bossis, G.; de Vicente, J., *Appl. Phys. Lett.*,**2013**,102,081907.
20. de Vicente, J.; Berli, C. L. A., *Rheol. Acta*,**2013**,DOI 10.1007/s00397-013-0704-8.
21. Klingenberg, D. J.; Zukoski, C. F., *Langmuir*,**1990**,6, 15.
22. Martin, J. E.; Anderson, R. A., *J. Chem. Phys.*,**1996**,*104(12)*,4814–4827.
23. de Gans, B. J.; Hoekstra, H.; Mellema, J., *Faraday Discuss.*,**1999**,*112*, 209–224.
24. Volkova,O.; Bossis, G.; Guyot, M.; Bashtovoi, V.; Reks, A., *J. Rheol.*,**2000**,*44*,91–104.
25. de Vicente, J.; Lopez-Lopez, M.; Durán, J. D.; Gonzalez-Caballero, F., *Rheol. Acta*,**2004**,*44*,94–103.
26. Marshall, L.; Zukoski, C. F.; Goodwin, J., *J. Chem. Soc., Faraday Trans.*,**1989**,*85*,2785-2795.
27. Felt, D. W.; Hagenbuchle, M.; Liu, J.; Richard, J., *J. Intel. Mat. Syst. Str.*,**1996**,*7*,589-593.
28. Ramos, J.; Klingenberg, D. J.; Hidalgo-Álvarez, R.; de Vicente, J., *J. Rheol.*,**2011**,*55(1)*,127-152.
29. Ginder, J. M.; Davis, L. C.; Elie, L. D. (**1996**) In Proceedings of the 5th International Conference on ER fluids, MR suspensions and Associated Technology, Bullough WA (ed), World Scientific, Singapore, p505.

30. Jordan, T. C.; Shaw, M. T.; McLeish, T. C. B., *J. Rheol,***1992**,*36*,441.
31. Parthasarathy, M.; Klingenberg, D. J., *Mater Sci. Eng* R, **1996**,*17*,57.
32. Carlson, D. J., *Journal of Intelligent Material Systems and Structures*,**2002**,*13*,431-435.
33. Private communication Lord Corporation.
34. de Vicente, J.; Bombard, A. J. F., in Magnetorheology: Advances and Applications; Wereley N., Ed.; Royal Society of Chemistry, **2013**.
35. Whittle, M., *J. Non-Newtonian Fluid Mech.*,**1990**,*37*,233.
36. Klingenberg, D. J., *J. Rheol.*,**1993**,*37*,199.
37. Parthasarathy, M.; Klingenberg, D. J.; van Swol, F.; Zukoski, C. F., *J. Chem. Phys.*,**1991**,*94*,6160.
38. Klingenberg, D. J., *Rheol. Acta*,**1995**,*34*,417.
39. Frenkel, D.; Smit, B., Understanding Molecular Simulation: from Algorithms to Applications, Academic Press: San Diego, **1996**.
40. Wang, Z.; Lin, Z.; Tao, R., *International Journal of Modern Physics B*,**1996**,*10*,1153.
41. Wang, Z.; Lin, Z.; Tao, R., *Chin. Phys. Lett.*,**1997**,*14*,151.
42. Wang, Z.; Lin, Z.; Fang, H.; Tao, R., *J. Appl. Phys.*,**1998**,*83*,1125.
43. de Vicente, J.; Gonzalez-Caballero, F.; Bossis, G.; Volkova, O., *J. Rheol.*,**2002**,*46*,1295-1303.
44. See, H.; Tanner, R., *Rheol. Acta,***2003**,*42*,166-170.
45. Laun, H. M.; Gabriel, C.; Schmidt, G., *J. Non-Newtonian Fluid Mech.,***2008**,*148*,47-56.
46. Gong, X.; Chaoyang, G.; Shouhu, X.; Taixiang, L.; Luhang, Z.; Peng, C., *Soft Matter,***2012**,*8*,5256-5261.
47. Ashour, O.; Rogers, C. A.; Kordonsky, W., *Journal of Intelligent Material Systems and Structures*,**1996**,*7*,123-130.
48. Olabi, A. G.; Grunwald, A., *Materials and Design,* **2007**,*28*,2658-2664.
49. See, H., *Rheol. Acta,***2003**,*42*,86–92.
50. Zhang, X. Z.; Gong, X. L.; Zhang, P. Q.; Wang, Q. M., *J. Appl. Phys.,***2004**,*96*,2359–2364.
51. Wang, X.; Gordaninejad, F., *Rheol. Acta,***2006**,*45*,899–908.
52. Mazlan, S. A.; Ekreem, K. H.; Olabi, A. G., *J. Mater. Process. Technol.,***2008**,*201*,780–785.
53. de Vicente, J.; Ruiz-López, J. A.; Andablo-Reyes, E.; Segovia-Gutiérrez, J. P.; Hidalgo-Álvarez, R., *J. Rheol.*,**2011**,*55*,753-779.
54. Ruiz-López, J. A.; Hidalgo-Álvarez, R.; de Vicente, J., *Rheol. Acta*,**2012**,*51*,595-602.
55. Ruiz-López, J. A.; Hidalgo-Álvarez, R.; de Vicente, J., *Journal of Physics: Conference Series*,**2013**,*412*,012057.